arXiv:1210.2366v2 [hep-ex] 3 Jan 2013

Measurement of the B_c^- meson lifetime in the decay $B_c^- \to J/\psi\ \pi^-$

T. Aaltonen,[21] B. Álvarez González[z],[9] S. Amerio,[40] D. Amidei,[32] A. Anastassov[x],[15] A. Annovi,[17] J. Antos,[12] G. Apollinari,[15] J.A. Appel,[15] T. Arisawa,[54] A. Artikov,[13] J. Asaadi,[49] W. Ashmanskas,[15] B. Auerbach,[57] A. Aurisano,[49] F. Azfar,[39] W. Badgett,[15] T. Bae,[25] A. Barbaro-Galtieri,[26] V.E. Barnes,[44] B.A. Barnett,[23] P. Barria[hh],[42] P. Bartos,[12] M. Bauce[ff],[40] F. Bedeschi,[42] S. Behari,[23] G. Bellettini[gg],[42] J. Bellinger,[56] D. Benjamin,[14] A. Beretvas,[15] A. Bhatti,[46] D. Bisello[ff],[40] I. Bizjak,[28] K.R. Bland,[5] B. Blumenfeld,[23] A. Bocci,[14] A. Bodek,[45] D. Bortoletto,[44] J. Boudreau,[43] A. Boveia,[11] L. Brigliadori[ee],[6] C. Bromberg,[33] E. Brucken,[21] J. Budagov,[13] H.S. Budd,[45] K. Burkett,[15] G. Busetto[ff],[40] P. Bussey,[19] A. Buzatu,[31] A. Calamba,[10] C. Calancha,[29] S. Camarda,[4] M. Campanelli,[28] M. Campbell,[32] F. Canelli,[11,15] B. Carls,[22] D. Carlsmith,[56] R. Carosi,[42] S. Carrillo[m],[16] S. Carron,[15] B. Casal[k],[9] M. Casarsa,[50] A. Castro[ee],[6] P. Catastini,[20] D. Cauz,[50] V. Cavaliere,[22] M. Cavalli-Sforza,[4] A. Cerri[f],[26] L. Cerrito[s],[28] Y.C. Chen,[1] M. Chertok,[7] G. Chiarelli,[42] G. Chlachidze,[15] F. Chlebana,[15] K. Cho,[25] D. Chokheli,[13] W.H. Chung,[56] Y.S. Chung,[45] M.A. Ciocci[hh],[42] A. Clark,[18] C. Clarke,[55] G. Compostella[ff],[40] M.E. Convery,[15] J. Conway,[7] M.Corbo,[15] M. Cordelli,[17] C.A. Cox,[7] D.J. Cox,[7] F. Crescioli[gg],[42] J. Cuevas[z],[9] R. Culbertson,[15] D. Dagenhart,[15] N. d'Ascenzo[w],[15] M. Datta,[15] P. de Barbaro,[45] M. Dell'Orso[gg],[42] L. Demortier,[46] M. Deninno,[6] F. Devoto,[21] M. d'Errico[ff],[40] A. Di Canto[gg],[42] B. Di Ruzza,[15] J.R. Dittmann,[5] M. D'Onofrio,[27] S. Donati[gg],[42] P. Dong,[15] M. Dorigo,[50] T. Dorigo,[40] K. Ebina,[54] A. Elagin,[49] A. Eppig,[32] R. Erbacher,[7] S. Errede,[22] N. Ershaidat[dd],[15] R. Eusebi,[49] S. Farrington,[39] M. Feindt,[24] J.P. Fernandez,[29] R. Field,[16] G. Flanagan[u],[15] R. Forrest,[7] M.J. Frank,[5] M. Franklin,[20] J.C. Freeman,[15] Y. Funakoshi,[54] I. Furic,[16] M. Gallinaro,[46] J.E. Garcia,[18] A.F. Garfinkel,[44] P. Garosi[hh],[42] H. Gerberich,[22] E. Gerchtein,[15] S. Giagu,[47] V. Giakoumopoulou,[3] P. Giannetti,[42] K. Gibson,[43] C.M. Ginsburg,[15] N. Giokaris,[3] P. Giromini,[17] G. Giurgiu,[23] V. Glagolev,[13] D. Glenzinski,[15] M. Gold,[35] D. Goldin,[49] N. Goldschmidt,[16] A. Golossanov,[15] G. Gomez,[9] G. Gomez-Ceballos,[30] M. Goncharov,[30] O. González,[29] I. Gorelov,[35] A.T. Goshaw,[14] K. Goulianos,[46] S. Grinstein,[4] C. Grosso-Pilcher,[11] R.C. Group[53],[15] J. Guimaraes da Costa,[20] S.R. Hahn,[15] E. Halkiadakis,[48] A. Hamaguchi,[38] J.Y. Han,[45] F. Happacher,[17] K. Hara,[51] D. Hare,[48] M. Hare,[52] R.F. Harr,[55] K. Hatakeyama,[5] C. Hays,[39] M. Heck,[24] J. Heinrich,[41] M. Herndon,[56] S. Hewamanage,[5] A. Hocker,[15] W. Hopkins[g],[15] D. Horn,[24] S. Hou,[1] R.E. Hughes,[36] M. Hurwitz,[11] U. Husemann,[57] N. Hussain,[31] M. Hussein,[33] J. Huston,[33] G. Introzzi,[42] M. Iori[jj],[47] A. Ivanov[p],[7] E. James,[15] D. Jang,[10] B. Jayatilaka,[14] E.J. Jeon,[25] S. Jindariani,[15] M. Jones,[44] K.K. Joo,[25] S.Y. Jun,[10] T.R. Junk,[15] T. Kamon[25],[49] P.E. Karchin,[55] A. Kasmi,[5] Y. Kato[o],[38] W. Ketchum,[11] J. Keung,[41] V. Khotilovich,[49] B. Kilminster,[15] D.H. Kim,[25] H.S. Kim,[25] J.E. Kim,[25] M.J. Kim,[17] S.B. Kim,[25] S.H. Kim,[51] Y.K. Kim,[11] Y.J. Kim,[25] N. Kimura,[54] M. Kirby,[15] S. Klimenko,[16] K. Knoepfel,[15] K. Kondo,[54] D.J. Kong,[25] J. Konigsberg,[16] A.V. Kotwal,[14] M. Kreps,[24] J. Kroll,[41] D. Krop,[11] M. Kruse,[14] V. Krutelyov[c],[49] T. Kuhr,[24] M. Kurata,[51] S. Kwang,[11] A.T. Laasanen,[44] S. Lami,[42] S. Lammel,[15] M. Lancaster,[28] R.L. Lander,[7] K. Lannon[y],[36] A. Lath,[48] G. Latino[hh],[42] T. LeCompte,[2] E. Lee,[49] H.S. Lee[q],[11] J.S. Lee,[25] S.W. Lee[bb],[49] S. Leo[gg],[42] S. Leone,[42] J.D. Lewis,[15] A. Limosani[t],[14] C.-J. Lin,[26] M. Lindgren,[15] E. Lipeles,[41] A. Lister,[18] D.O. Litvintsev,[15] C. Liu,[43] H. Liu,[53] Q. Liu,[44] T. Liu,[15] S. Lockwitz,[57] A. Loginov,[57] D. Lucchesi[ff],[40] J. Lueck,[24] P. Lujan,[26] P. Lukens,[15] G. Lungu,[46] J. Lys,[26] R. Lysak[e],[12] R. Madrak,[15] K. Maeshima,[15] P. Maestro[hh],[42] S. Malik,[46] G. Manca[a],[27] A. Manousakis-Katsikakis,[3] F. Margaroli,[47] C. Marino,[24] M. Martínez,[4] P. Mastrandrea,[47] K. Matera,[22] M.E. Mattson,[55] A. Mazzacane,[15] P. Mazzanti,[6] K.S. McFarland,[45] P. McIntyre,[49] R. McNulty[j],[27] A. Mehta,[27] P. Mehtala,[21] C. Mesropian,[46] T. Miao,[15] D. Mietlicki,[32] A. Mitra,[1] H. Miyake,[51] S. Moed,[15] N. Moggi,[6] M.N. Mondragon[m],[15] C.S. Moon,[25] R. Moore,[15] M.J. Morello[ii],[42] J. Morlock,[24] P. Movilla Fernandez,[15] A. Mukherjee,[15] Th. Muller,[24] P. Murat,[15] M. Mussini[ee],[6] J. Nachtman[n],[15] Y. Nagai,[51] J. Naganoma,[54] I. Nakano,[37] A. Napier,[52] J. Nett,[49] C. Neu,[53] M.S. Neubauer,[22] J. Nielsen[d],[26] L. Nodulman,[2] S.Y. Noh,[25] O. Norniella,[22] L. Oakes,[39] S.H. Oh,[14] Y.D. Oh,[25] I. Oksuzian,[53] T. Okusawa,[38] R. Orava,[21] L. Ortolan,[4] S. Pagan Griso[ff],[40] C. Pagliarone,[50] E. Palencia[f],[9] V. Papadimitriou,[15] A.A. Paramonov,[2] J. Patrick,[15] G. Pauletta[kk],[50] M. Paulini,[10] C. Paus,[30] D.E. Pellett,[7] A. Penzo,[50] T.J. Phillips,[14] G. Piacentino,[42] E. Pianori,[41] J. Pilot,[36] K. Pitts,[22] C. Plager,[8] L. Pondrom,[56] S. Poprocki[g],[15] K. Potamianos,[44] F. Prokoshin[cc],[13] A. Pranko,[26] F. Ptohos[h],[17] G. Punzi[gg],[42] A. Rahaman,[43] V. Ramakrishnan,[56] N. Ranjan,[44] I. Redondo,[29] P. Renton,[39] M. Rescigno,[47] T. Riddick,[28] F. Rimondi[ee],[6] L. Ristori[42],[15] A. Robson,[19] T. Rodrigo,[9] T. Rodriguez,[41] E. Rogers,[22] S. Rolli[i],[52] R. Roser,[15] F. Ruffini[hh],[42] A. Ruiz,[9] J. Russ,[10] V. Rusu,[15] A. Safonov,[49] W.K. Sakumoto,[45] Y. Sakurai,[54] L. Santi[kk],[50] K. Sato,[51] V. Saveliev[w],[15] A. Savoy-Navarro[aa],[15] P. Schlabach,[15] A. Schmidt,[24] E.E. Schmidt,[15] T. Schwarz,[15] L. Scodellaro,[9] A. Scribano[hh],[42] F. Scuri,[42] S. Seidel,[35] Y. Seiya,[38] A. Semenov,[13] F. Sforza[hh],[42] S.Z. Shalhout,[7] T. Shears,[27] P.F. Shepard,[43] M. Shimojima[v],[51] M. Shochet,[11] I. Shreyber-Tecker,[34] A. Simonenko,[13] P. Sinervo,[31] K. Sliwa,[52] J.R. Smith,[7] F.D. Snider,[15] A. Soha,[15] V. Sorin,[4] H. Song,[43] P. Squillacioti[hh],[42] M. Stancari,[15] R. St. Denis,[19]

B. Stelzer,[31] O. Stelzer-Chilton,[31] D. Stentz[x],[15] J. Strologas,[35] G.L. Strycker,[32] Y. Sudo,[51] A. Sukhanov,[15] I. Suslov,[13] K. Takemasa,[51] Y. Takeuchi,[51] J. Tang,[11] M. Tecchio,[32] P.K. Teng,[1] J. Thom[g],[15] J. Thome,[10] G.A. Thompson,[22] E. Thomson,[41] D. Toback,[49] S. Tokar,[12] K. Tollefson,[33] T. Tomura,[51] D. Tonelli,[15] S. Torre,[17] D. Torretta,[15] P. Totaro,[40] M. Trovato[ii],[42] F. Ukegawa,[51] S. Uozumi,[25] A. Varganov,[32] F. Vázquez[m],[16] G. Velev,[15] C. Vellidis,[15] M. Vidal,[44] I. Vila,[9] R. Vilar,[9] J. Vizán,[9] M. Vogel,[35] G. Volpi,[17] P. Wagner,[41] R.L. Wagner,[15] T. Wakisaka,[38] R. Wallny,[8] S.M. Wang,[1] A. Warburton,[31] D. Waters,[28] W.C. Wester III,[15] D. Whiteson[b],[41] A.B. Wicklund,[2] E. Wicklund,[15] S. Wilbur,[11] F. Wick,[24] H.H. Williams,[41] J.S. Wilson,[36] P. Wilson,[15] B.L. Winer,[36] P. Wittich[g],[15] S. Wolbers,[15] H. Wolfe,[36] T. Wright,[32] X. Wu,[18] Z. Wu,[5] K. Yamamoto,[38] D. Yamato,[38] T. Yang,[15] U.K. Yang[r],[11] Y.C. Yang,[25] W.-M. Yao,[26] G.P. Yeh,[15] K. Yi[n],[15] J. Yoh,[15] K. Yorita,[54] T. Yoshida[l],[38] G.B. Yu,[14] I. Yu,[25] S.S. Yu,[15] J.C. Yun,[15] A. Zanetti,[50] Y. Zeng,[14] C. Zhou,[14] and S. Zucchelli[ee6]

(CDF Collaboration)

[1] *Institute of Physics, Academia Sinica, Taipei, Taiwan 11529, Republic of China*
[2] *Argonne National Laboratory, Argonne, Illinois 60439, USA*
[3] *University of Athens, 157 71 Athens, Greece*
[4] *Institut de Fisica d'Altes Energies, ICREA, Universitat Autonoma de Barcelona, E-08193, Bellaterra (Barcelona), Spain*
[5] *Baylor University, Waco, Texas 76798, USA*
[6] *Istituto Nazionale di Fisica Nucleare Bologna, [ee] University of Bologna, I-40127 Bologna, Italy*
[7] *University of California, Davis, Davis, California 95616, USA*
[8] *University of California, Los Angeles, Los Angeles, California 90024, USA*
[9] *Instituto de Fisica de Cantabria, CSIC-University of Cantabria, 39005 Santander, Spain*
[10] *Carnegie Mellon University, Pittsburgh, Pennsylvania 15213, USA*
[11] *Enrico Fermi Institute, University of Chicago, Chicago, Illinois 60637, USA*
[12] *Comenius University, 842 48 Bratislava, Slovakia; Institute of Experimental Physics, 040 01 Kosice, Slovakia*
[13] *Joint Institute for Nuclear Research, RU-141980 Dubna, Russia*
[14] *Duke University, Durham, North Carolina 27708, USA*
[15] *Fermi National Accelerator Laboratory, Batavia, Illinois 60510, USA*
[16] *University of Florida, Gainesville, Florida 32611, USA*
[17] *Laboratori Nazionali di Frascati, Istituto Nazionale di Fisica Nucleare, I-00044 Frascati, Italy*
[18] *University of Geneva, CH-1211 Geneva 4, Switzerland*
[19] *Glasgow University, Glasgow G12 8QQ, United Kingdom*
[20] *Harvard University, Cambridge, Massachusetts 02138, USA*
[21] *Division of High Energy Physics, Department of Physics,*
University of Helsinki and Helsinki Institute of Physics, FIN-00014, Helsinki, Finland
[22] *University of Illinois, Urbana, Illinois 61801, USA*
[23] *The Johns Hopkins University, Baltimore, Maryland 21218, USA*
[24] *Institut für Experimentelle Kernphysik, Karlsruhe Institute of Technology, D-76131 Karlsruhe, Germany*
[25] *Center for High Energy Physics: Kyungpook National University,*
Daegu 702-701, Korea; Seoul National University, Seoul 151-742,
Korea; Sungkyunkwan University, Suwon 440-746,
Korea; Korea Institute of Science and Technology Information,
Daejeon 305-806, Korea; Chonnam National University, Gwangju 500-757,
Korea; Chonbuk National University, Jeonju 561-756, Korea
[26] *Ernest Orlando Lawrence Berkeley National Laboratory, Berkeley, California 94720, USA*
[27] *University of Liverpool, Liverpool L69 7ZE, United Kingdom*
[28] *University College London, London WC1E 6BT, United Kingdom*
[29] *Centro de Investigaciones Energeticas Medioambientales y Tecnologicas, E-28040 Madrid, Spain*
[30] *Massachusetts Institute of Technology, Cambridge, Massachusetts 02139, USA*
[31] *Institute of Particle Physics: McGill University, Montréal, Québec,*
Canada H3A 2T8; Simon Fraser University, Burnaby, British Columbia,
Canada V5A 1S6; University of Toronto, Toronto, Ontario,
Canada M5S 1A7; and TRIUMF, Vancouver, British Columbia, Canada V6T 2A3
[32] *University of Michigan, Ann Arbor, Michigan 48109, USA*
[33] *Michigan State University, East Lansing, Michigan 48824, USA*
[34] *Institution for Theoretical and Experimental Physics, ITEP, Moscow 117259, Russia*
[35] *University of New Mexico, Albuquerque, New Mexico 87131, USA*
[36] *The Ohio State University, Columbus, Ohio 43210, USA*
[37] *Okayama University, Okayama 700-8530, Japan*
[38] *Osaka City University, Osaka 588, Japan*
[39] *University of Oxford, Oxford OX1 3RH, United Kingdom*
[40] *Istituto Nazionale di Fisica Nucleare, Sezione di Padova-Trento, [ff] University of Padova, I-35131 Padova, Italy*
[41] *University of Pennsylvania, Philadelphia, Pennsylvania 19104, USA*

[42] Istituto Nazionale di Fisica Nucleare Pisa, [gg] University of Pisa,
[hh] University of Siena and [ii] Scuola Normale Superiore, I-56127 Pisa, Italy
[43] University of Pittsburgh, Pittsburgh, Pennsylvania 15260, USA
[44] Purdue University, West Lafayette, Indiana 47907, USA
[45] University of Rochester, Rochester, New York 14627, USA
[46] The Rockefeller University, New York, New York 10065, USA
[47] Istituto Nazionale di Fisica Nucleare, Sezione di Roma 1,
[jj] Sapienza Università di Roma, I-00185 Roma, Italy
[48] Rutgers University, Piscataway, New Jersey 08855, USA
[49] Texas A&M University, College Station, Texas 77843, USA
[50] Istituto Nazionale di Fisica Nucleare Trieste/Udine,
I-34100 Trieste, [kk] University of Udine, I-33100 Udine, Italy
[51] University of Tsukuba, Tsukuba, Ibaraki 305, Japan
[52] Tufts University, Medford, Massachusetts 02155, USA
[53] University of Virginia, Charlottesville, Virginia 22906, USA
[54] Waseda University, Tokyo 169, Japan
[55] Wayne State University, Detroit, Michigan 48201, USA
[56] University of Wisconsin, Madison, Wisconsin 53706, USA
[57] Yale University, New Haven, Connecticut 06520, USA

(Dated: January 4, 2013)

The lifetime of the B_c^- meson is measured using 272 exclusive $B_c^- \to J/\psi(\to \mu^+\mu^-)\,\pi^-$ decays reconstructed in data from proton-antiproton collisions corresponding to an integrated luminosity of 6.7 fb^{-1} recorded by the CDF II detector at the Fermilab Tevatron. The lifetime of the B_c^- meson is measured to be $\tau(B_c^-) = 0.452 \pm 0.048(\text{stat}) \pm 0.027(\text{syst})$ ps. This is the first measurement of the B_c^- meson lifetime in a fully-reconstructed hadronic channel, and it agrees with previous results and has comparable precision.

PACS numbers: 14.40.Nd, 13.25.Hw

In the standard model the B_c^- meson is the only meson composed of two distinct heavy quarks. The B_c^- meson decay can be governed by the decay of the b or $\overline{c}$ spectator quarks or can proceed through the annihilation of the b and $\overline{c}$ quarks. Various theoretical techniques have been used to predict the B_c^- meson lifetime. An operator-product-expansion calculation [1] predicts a B_c^- meson lifetime in the range of 0.4 to 0.7 ps. A QCD sum rule approach [2] predicts the lifetime to be 0.48 ± 0.05 ps. Another approach [3], estimating the B_c^- meson lifetime by global fitting of the phenomenological parameters of all other heavy mesons, gives a result of 0.36 or 0.47 ps, depending on different choices of effective heavy-quark masses.

The B_c^- meson lifetime was measured previously in semileptonic decays by CDF [4] and D0 [5]. These measurements have an undetected neutrino in the final state and rely on the modeling of the B_c^- meson momentum to account for unmeasured momentum of the neutrino. Therefore, a measurement of the B_c^- meson lifetime in a fully-reconstructed decay mode is desired since it does not suffer from this limitation. CDF is the first experiment to observe the fully-reconstructed $B_c^- \to J/\psi(\to \mu^+\mu^-)\,\pi^-$ decay mode [6] and to measure the B_c^- mass [7]. In this paper we present a lifetime measurement of the B_c^- meson using this decay mode. This measurement is made using data from $p\overline{p}$ collisions at a center-of-mass energy of 1.96 TeV recorded by the CDF II detector. The results are based on a data sample with an integrated luminosity of 6.7 fb^{-1}.

The components of the CDF II detector [8] most relevant for this analysis are the charged-particle tracking and muon identification systems. The tracking system is immersed in a uniform 1.4 T solenoidal magnetic field coaxial with the beam line, and consists of single- and double-sided silicon detectors [9] and a 96-layer open-cell drift chamber (COT) [10]. The muon system is used to identify the $J/\psi \to \mu^+\,\mu^-$ decay. Two sets of muon chambers [11, 12] are used to cover different pseudorapidity regions.

A three-level event-selection system (trigger) is used to collect events enriched in $J/\psi \to \mu^+\,\mu^-$ decays [8]. The event reconstruction starts by combining two muon candidates to form a J/ψ candidate. The trigger requirements are confirmed by selecting events that contain two oppositely charged muon candidates, each with matching COT and muon chamber tracks. The muon-pair mass is required to be within 80 MeV/c^2 of the world-average J/ψ mass [13], where the mass resolution is 13 MeV/c^2.

Both $J/\psi\,K^-$ and $J/\psi\,\pi^-$ combinations are reconstructed in this analysis. The large $B^- \to J/\psi\,K^-$ sample is used as a reference decay for $B_c^- \to J/\psi\,\pi^-$. These final states are identified by assigning the K^- or π^- mass to other reconstructed tracks not used in the J/ψ candidates and forming B^- or B_c^- candidates. Each three-track combination must satisfy a kinematic fit in which the three tracks are required to originate from a common decay point, and the invariant mass of the muon pair is constrained to the world-average J/ψ mass [13]. The K^- and π^- candidate track is named the third track

h^-. A minimal selection is made on kinematic quantities after the constrained fit including $p_T(h^-) > 1.7$ GeV/c and $p_T(B) > 5$ GeV/c, where p_T is the momentum component transverse to the beam line, and B refers to a $J/\psi\ h^-$ candidate. The selection criteria for the B candidates are listed in Table I and discussed below.

TABLE I. Selection requirements.

Selection variable	Requirement
$p_T(h^-)$	> 2.0 GeV/c
$p_T(B)$	> 6.5 GeV/c
$P(\chi^2)$	$> 0.1\%$
$\lvert d(B)\rvert/\sigma_{d(B)}$	< 2.0
β_T	< 0.2 radians
I_B	> 0.6
$\sigma_m(B)$	< 40 MeV/c^2
ct	> 80 μm
$\sigma_{ct}(B)$	$< \max[35, 65 - 3\ p_T(B)(\mathrm{GeV}/c)]$ μm

The h^- and B candidates are required to have a minimum p_T to suppress combinatorial background events. We reject events with poorly defined decay points by imposing a lower threshold to the chi-square probability $P(\chi^2)$ of the constrained fit used to reconstruct the B candidates. We select B candidates that originate from the primary interaction point by requiring a small impact parameter $d(B)$ (transverse distance of closest approach to the beam line) in units of its uncertainty $\sigma_{d(B)}$ and a small angle β_T between $\vec{L}_T$ and $\vec{p}_T(B)$, where $\vec{L}_T$ is the transverse displacement vector from the primary interaction point to the B-decay point, and $\vec{p}_T(B)$ denotes a vector in the transverse plane along the momentum direction of the B candidate. The isolation I_B of the B candidate is defined as $I_B \equiv p(B)/(p(B) + |\sum_i \vec{p}_i|)$, where $\sum_i \vec{p}_i$ is the sum of momenta over all other reconstructed tracks not used in the $J/\psi\ h^-$ combination within $\sqrt{(\Delta\eta)^2 + (\Delta\phi)^2} < 0.7$, and $\Delta\eta$ and $\Delta\phi$ are the differences in pseudorapidities and azimuthal angles of tracks relative to $\vec{p}(B)$. We also suppress the promptly produced combinatorial background by rejecting candidates with small ct, where ct is the decay length of the B candidate determined by

$$ct \equiv \vec{L}_T \cdot \vec{p}_T(B) \frac{c\ m(B)}{|p_T(B)|^2}, \qquad (1)$$

and $m(B)$ is the reconstructed mass of the B candidate. Requirements on $\sigma_m(B)$ and $\sigma_{ct}(B)$ are made to reject poorly reconstructed events, where $\sigma_m(B)$ and $\sigma_{ct}(B)$ are the associated uncertainties from the kinematic fit of $m(B)$ and $ct(B)$, respectively. The optimization of the selection requirements is obtained by maximizing the quantity $\mathcal{S}/\sqrt{(\mathcal{S}+\mathcal{B})}$ where the background $\mathcal{B}$ is estimated from the mass sidebands in data and the signal $\mathcal{S}$ is estimated from the signal-region data after subtracting background contributions as calculated from sidebands.

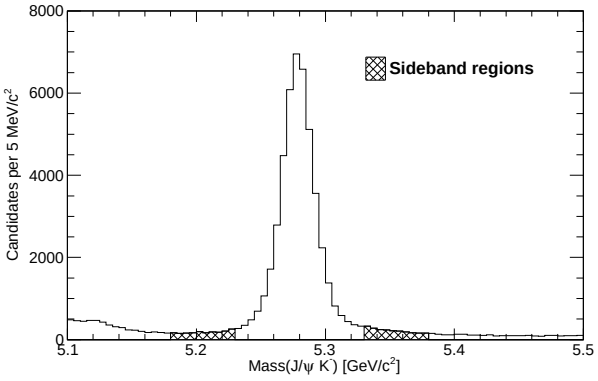

FIG. 1. Invariant-mass distribution of $J/\psi\ K^-$ candidates. The hatched areas are the sideband regions and the signal region lies between them.

Because the $\sigma_{ct}(B)$ distribution depends on $p_T(B)$, we vary the requirement on $\sigma_{ct}(B)$ as a function of $p_T(B)$. For candidates with $p_T(B) < 10$ GeV/c, we require $\sigma_{ct}(B) < (65 - 3\ p_T(B))$ μm for $p_T(B)$ measured in GeV/c, and $\sigma_{ct}(B) < 35$ μm for $p_T(B) \geq 10$ GeV/c. This p_T-dependent requirement on $\sigma_{ct}(B)$ is chosen to be highly efficient for preserving signal while reducing combinatorial background and leads to no measurable biases.

The resulting B^- mass distribution is shown in Fig. 1. The signal region lies between two background sideband regions and has 46 280 B^- candidates. The two sideband regions consist of a lower sideband from 5.18 to 5.23 GeV/c^2 and an upper sideband from 5.33 to 5.38 GeV/c^2, as shown in the hatched areas.

The $B_c^- \to J/\psi\ \pi^-$ candidates are formed from the same parent sample as the $B^- \to J/\psi\ K^-$ candidates where the only change to the reconstruction is to assign the pion mass to the third track. We then select events for further analysis using the selections in Table I. The reconstructed mass distribution for the B_c^- candidates is shown in Fig. 2. The signal region lies between two background sideband regions and has 1496 B_c^- candidates. The two sideband regions of B_c^- candidates consist of a lower sideband from 6.16 to 6.21 GeV/c^2 and an upper sideband from 6.33 to 6.60 GeV/c^2, as shown in the hatched areas. The lower sideband is narrow to avoid contamination from semileptonic B_c^- decays where the lepton is misidentified as a pion.

We generate Monte Carlo simulations for $B^- \to J/\psi\ K^-$ and $B_c^- \to J/\psi\ \pi^-$ decays to study the efficiency of the selection criteria as a function of decay length. The Fixed-Order plus Next-to-Leading Logarithms (FONLL) p_T spectrum [14] is used for the B^- production spectrum. We use the calculation of Ref [15] as the spectrum for B_c^- simulation. In comparing the FONLL p_T spectrum for B^- production with the experimental data, reasonable consistency is

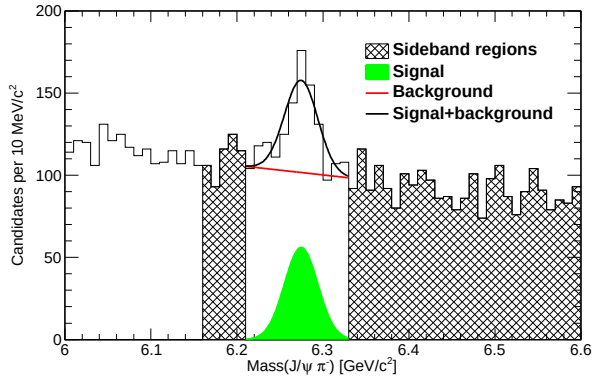

FIG. 2. Invariant-mass distribution of $J/\psi\ \pi^-$ candidates. The hatched areas are the sideband regions and the signal region lies between them. The fit result is overlaid in the signal region, as well as the signal and background components.

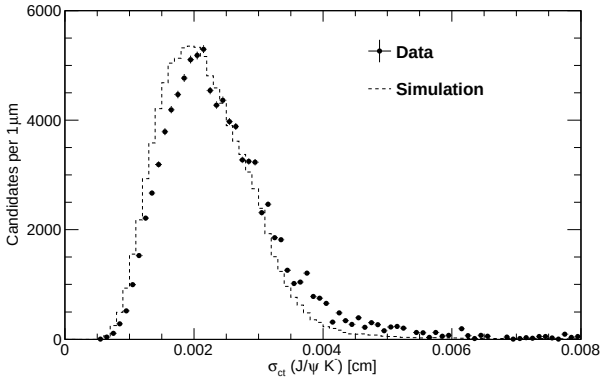

FIG. 3. The σ_{ct} distribution of $J/\psi\ K^-$ candidates obtained from the simulation is compared with data.

observed for $p_T > 6$ GeV/c, and any residual discrepancy gives a negligible systematic uncertainty. To further validate the $B^- \to J/\psi\ K^-$ simulation, we compare the distributions of the selection variables listed in Table I for experimental data and simulation. Generally, good agreement is observed for all selection variables except for $\sigma_{ct}(B)$, whose comparison is shown in Fig. 3. The disagreement in the $\sigma_{ct}(B)$ distribution arises from mis-modeling of the silicon tracking detector in the simulation, giving a smaller $\sigma_{ct}(B)$ compared with experimental data for a given $p_T(B)$. Consequently, the selection requirement made on $\sigma_{ct}(B)$ for simulation is tuned in order to allow the same efficiency as in the experimental data. These $\sigma_{ct}(B)$ selection values for simulation are also p_T-dependent, and the p_T threshold remains the same; the only change is to require $\sigma_{ct}(B) < (45 - 2\ p_T(B))\ \mu$m for $p_T(B) < 10$ GeV/c,

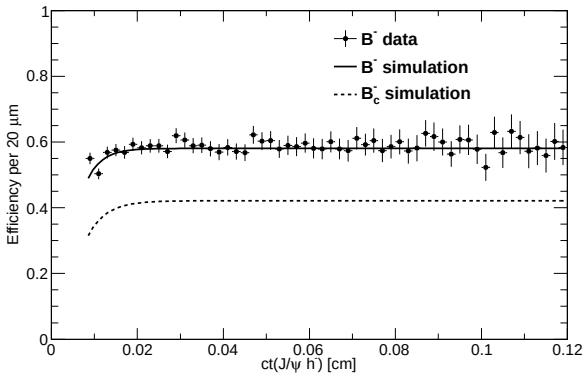

FIG. 4. Comparison of efficiency for $B^- \to J/\psi\ K^-$ obtained from data and the fit result from simulation. Also shown is the fit result for $B_c^- \to J/\psi\ \pi^-$ simulation.

and $\sigma_{ct}(B) < 25\ \mu$m for $p_T(B) \geq 10$ GeV/c. The systematic uncertainty associated with the tuning will be discussed later.

The efficiency of the selection criteria is found by comparing the decay-length distribution after applying the selection in Table I to that obtained from the minimal selection which requires $p_T(h^-) > 1.7$ GeV/c and $p_T(B) > 5$ GeV/c. The efficiency determined from simulation is then fit to a function of the form

$$\epsilon(ct) = C\left[1 - \exp\left(\frac{a - ct}{b}\right)\right], \qquad (2)$$

where C, a, b are parameters to be fit. Figure 4 shows the efficiency determined from $B^- \to J/\psi\ K^-$ experimental data as well as the fit result from simulation. The parameter C in Eq. (2) is not necessary in the lifetime fit because only the relative shape of the efficiency function matters. The requirement on β_T leads to an efficiency that is not constant as a function of decay length. This variable is very effective in rejecting background events, especially for events with small ct. The good agreement between the simulated efficiency and the data-determined efficiency supports the use of this approach in the ct-dependent efficiency. The efficiency for the $B_c^- \to J/\psi\ \pi^-$ decay as a function of decay time determined from simulation is fit and also shown in Fig. 4.

We use a maximum log-likelihood simultaneous fit to the unbinned mass and decay-length distributions of the B_c^- candidates. The likelihood function consists of signal and background parts, and each part has a mass term and a decay length term. The log-likelihood function is

$$\ln \mathcal{L} = \sum_i \ln \left[f_s \; M_s(m_i) \; T_s(ct_i) + (1 - f_s) \; M_b(m_i) \; T_b(ct_i) \right], \quad (3)$$

where f_s is the signal fraction, m_i and ct_i are the reconstructed mass and decay length for event i. $M_s(m_i)$ and $T_s(ct_i)$ are the normalized probability density functions for mass and decay length of the signal model, and $M_b(m_i)$ and $T_b(ct_i)$ are the corresponding functions of the background model. The signal mass model $M_s(m_i)$ is described by a Gaussian distribution with mean m_0 and width σ_m, whose values are determined by the fit. The signal decay length model $T_s(ct_i)$ is an exponential distribution with characteristic lifetime τ, smeared by the detector resolution and multiplied by the efficiency function given in Eq. (2). The detector resolution, which is modeled as a Gaussian distribution centered at zero with a width of 20 μm, is chosen to be consistent with calibration using promptly decaying background events [16]. The background mass model $M_b(m_i)$ is described by a linear distribution, and $T_b(ct_i)$ is described by a linear combination of three exponential distributions.

A two-step process is used to extract the lifetime of the B_c^- meson. The first step includes the efficiency fit and the sideband fit. The efficiency fit is performed on the simulated events using Eq. (2), and the result is shown in Fig. 4. The sideband fit consists of two separate fits in the sideband regions. The first fit determines the background mass model parameters, and the second fit determines the background decay-time model parameters. The signal region is fit with the efficiency and background parameters Gaussian-constrained to the result of the earlier fits. The signal fraction and the signal model parameters are allowed to float freely in maximizing the log-likelihood function given in Eq. (3).

To validate this fitting technique, the fit is first applied to the B^- candidates shown in Fig. 1 to extract the B^- meson lifetime. The B^- lifetime which is found to be $\tau(B^-) = 1.637 \pm 0.010$ (stat) ps is in agreement with the world-average value of 1.641 ± 0.008 ps [13]. The B^- signal yield returned from the fit is $43\,308 \pm 171$. The fit is then applied to the B_c^- candidates shown in Fig. 2, resulting in a lifetime of $\tau(B_c^-) = 0.452 \pm 0.048$ (stat) ps for the B_c^- meson, which is taken as our central result, with a B_c^- signal yield of 272 ± 61 (stat) candidates. The B_c^- meson mass of 6274.6 ± 2.9 (stat) MeV/c^2 returned from the fit is in good agreement with the previous CDF determination [7]. Figures 2 and 5 show the distribution of the $J/\psi\ \pi^-$ mass and decay length. The fit projections are overlaid.

We have considered several sources of systematic uncertainty and evaluated their contributions. To evaluate possible systematic uncertainties with the models in the likelihood function, we generate 400 simulated data samples (pseudoexperiments) whose distributions are based on the fit results determined by the experimental data. These pseudoexperiments are then fit with the default and alternate models separately. The distributions of the sample-by-sample lifetime differences between different models are obtained and compared with the differences observed in experimental data. To assess the effect of the choice of the linear model for the mass-fit background, we compare to the result of a fit using a bilinear model that allows the background distribution to have different slopes at masses lower and higher than the B_c^- pole mass, with the constraint that these two distributions intersect at the fit B_c^- mass value. The fit lifetime with this bilinear model has a shift of –0.009 ps compared with the default linear model. The pseudoexperiments suggests up to a 0.017 ps difference from this variation. We conclude that the shift between the data fits is consistent with the spread among the pseudoexperiments, and we use that larger difference as the systematic uncertainty from the background mass model.

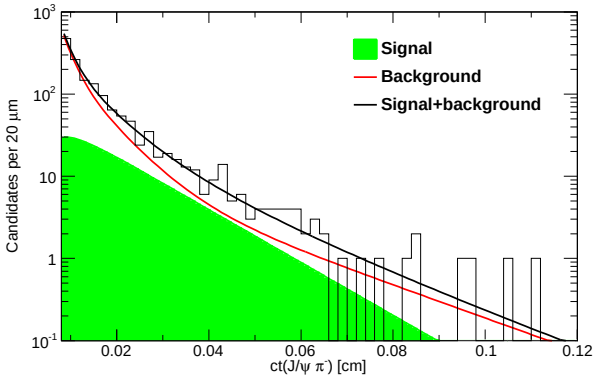

FIG. 5. Decay-length distribution of $J/\psi\ \pi^-$ candidates. The fit projection, along individual contributions from signal and background, is overlaid.

To assess a possible systematic uncertainty due to the modeling of the long tail in the background decay-length distribution, we test an alternate model of the background decay time which uses a linear distribution to replace the component with the largest characteristic lifetime in the three exponential distributions. This variation gives a lifetime result that changes by –0.0007 ps compared with the default background decay-time model. However, fit results from pseudoexperiments suggest the difference between these two models could be 0.013 ps, which is included as the systematic uncertainty due to the choice of the background decay-time model.

The signal decay-time model includes the efficiency determined from the simulation. We have performed several studies to estimate the associated systematic un-

certainty. First, the fit is repeated using an efficiency function obtained without tuning the $\sigma_{ct}(B)$ difference between data and simulation. The difference in the estimated lifetime is 0.003 ps. Second, the efficiency function is shifted toward lower and higher decay length by 20 μm to account for a possible uncertainty in determining the efficiency function parameters; this 20 μm shift is equivalent to three standard deviations of the parameter a in Eq. (2). This variation gives a difference of –0.010 (+0.007) ps for shifting toward lower (higher) decay lengths. The distribution of the difference between the resulting lifetimes in the pseudoexperiments is fit by a Gaussian distribution that centers at –0.006 (0.004) ps with a width of 0.002 (0.001) ps for shifting toward lower (higher) decay lengths. Third, the systematic uncertainty associated with the B_c^- production spectrum has been assessed. We vary the relative fraction of different contributions to the production spectrum; the difference in the corresponding efficiency is negligible and no systematic uncertainty is assigned to it. Finally, to further study the systematic uncertainty associated with the production spectrum, we use the efficiency parameters obtained from the $B^- \to J/\psi\ K^-$ simulation. Since the B^- production spectrum is quite different from that of B_c^-, the fit lifetime difference of 0.007 ps indicates that the production spectrum does not contribute significantly to the systematic uncertainty. Thus, the total systematic uncertainty associated with the signal decay-time model is taken to be 0.010 ps.

Correlations between the lifetime and other parameters of the analysis are considered as possible systematic uncertainties. The list of parameters includes the minimum and maximum decay length for events in the final fit, adding a parameter to the efficiency model, small variations in the sideband definitions, small modifications in the selection requirements, the use of an alternate fit procedure which fits the sideband and the signal regions simultaneously, the mass resolution in the signal model, the background fraction, and the three terms describing the exponentials in the background decay time model. No systematic effect was found to significantly exceed the variations expected from statistical uncertainties. We assign an additional uncertainty of 0.010 ps as a conservative approach to account for possible small systematic effects.

The systematic uncertainty due to tracking detector misalignments is evaluated by generating simulated samples with radial displacements of individual sensors as well as translation and rotation of the silicon detector relative to the COT [17]. A systematic uncertainty of 0.007 ps is assigned to the misalignment based on these simulated samples. The systematic uncertainty from the signal mass model is evaluated by including a contribution to the total B_c^- signal yield from the Cabibbo-suppressed decay $B_c^- \to J/\psi\ K^-$ in the signal mass shape. The Cabibbo-suppressed contribution is fixed to be 5% of the total B_c^- signal yield as determined from the Cabibbo angle. This effect results in a 0.003 ps variation.

The systematic uncertainty from the fitting technique itself is tested by generating pseudoexperiments, and comparing the fit lifetimes with the input lifetime. The bias on the lifetime returned by the fit is found to be no greater than 0.003 ps which we take as systematic uncertainty. Table II summarizes the systematic uncertainties, which are added in quadrature to determine the total systematic uncertainty.

TABLE II. Summary of systematic uncertainties.

Source	Uncertainty [ps]
Background mass model	0.017
Background decay-time model	0.013
Signal decay-time model	0.010
Correlation	0.010
Misalignment	0.007
Signal mass model	0.003
Fitting technique	0.003
Total	0.027

Given that the efficiency is not uniform over decay length, our result relies on the accuracy of the simulation in determining the efficiency. We check our result by measuring the B_c^- lifetime using a different set of selection criteria, each of which has uniform efficiency in the $B^- \to J/\psi\ K^-$ decay. The most important differences between these selection criteria and those listed in Table I are removing the β_T requirement and using a larger minimum ct requirement. The alternate selection criteria gives 6538 B_c^- candidates between 6.0 and 6.6 GeV/c^2 which is roughly the same number as obtained from the selections in Table I (6368 candidates), while only 2578 candidates are common to both samples.

The consistency check also uses an unbinned maximum log-likelihood fit to extract the B_c^- meson lifetime. The signal mass model consists of a Gaussian distribution centered at the B_c^- meson mass and a Cabibbo-suppressed $B_c^- \to J/\psi\ K^-$ Gaussian distribution centered at 60 MeV/c^2 below the B_c^- meson mass with a 30 MeV/c^2 width. The signal decay-time model is an exponential distribution convoluted with the detector resolution. The background mass model is described by a linear distribution, and the background decay-time model consists of two prompt Gaussian distributions, two positive exponential distributions, and one negative exponential distribution.

A similar two-step fit is used in the consistency check. The first step is to determine the background parameters from the sideband fit, where the sideband is defined as the $J/\psi\ \pi^-$ invariant-mass region between 6.4 and 6.5 GeV/c^2. The sideband fit is performed on events with decay length between –1000 μm and 1000 μm and the resulting background parameters are fixed in the second step. In the second step we fit events in the signal region between 6.16 and 6.36 GeV/c^2, and only the signal fraction and signal model parameters

are allowed to float. The consistency check is first performed on the B^- candidates. The fit result finds the B^- lifetime to be $\tau = 1.647 \pm 0.020$ (stat) ps, which agrees with the world-average value of 1.641 ± 0.008 ps [13]. The consistency check is then applied to the B_c^- candidates, giving a B_c^- meson lifetime of $\tau = 0.450 \pm 0.053$ (stat) ps which is consistent with our central value of 0.452 ± 0.048 (stat) ps. The B_c^- signal yield from the consistency check is 308 ± 39 (stat) which is compared with 272 ± 61 (stat) from the central result. The total systematic uncertainty in the consistency check is 0.033 ps where the largest uncertainty of 0.027 ps comes from the background decay-time model. Thus, we conclude that our central result obtained from the *ct*-dependent efficiency is reliable.

In conclusion, we have made the first measurement of the B_c^- meson lifetime in a fully-reconstructed hadronic decay mode. Using the $B_c^- \to J/\psi\, \pi^-$ decay channel, the lifetime of the B_c^- meson is measured to be $\tau = 0.452 \pm 0.048(\text{stat}) \pm 0.027(\text{syst})$ ps. This result is consistent with the most recent result from the D0 collaboration [5] using semileptonic decay channels, $\tau = 0.448\ ^{+0.038}_{-0.036}(\text{stat}) \pm 0.032(\text{syst})$ ps, and has comparable precision. The result also agrees with theoretical calculations in which the decay width of the B_c^- meson is dominated by the decay of the charm quark.

We thank the Fermilab staff and the technical staffs of the participating institutions for their vital contributions. This work was supported by the U.S. Department of Energy and National Science Foundation; the Italian Istituto Nazionale di Fisica Nucleare; the Ministry of Education, Culture, Sports, Science and Technology of Japan; the Natural Sciences and Engineering Research Council of Canada; the National Science Council of the Republic of China; the Swiss National Science Foundation; the A.P. Sloan Foundation; the Bundesministerium für Bildung und Forschung, Germany; the Korean World Class University Program, the National Research Foundation of Korea; the Science and Technology Facilities Council and the Royal Society, UK; the Russian Foundation for Basic Research; the Ministerio de Ciencia e Innovación, and Programa Consolider-Ingenio 2010, Spain; the Slovak R&D Agency; the Academy of Finland; and the Australian Research Council (ARC).

[1] M. Beneke and G. Buchalla, Phys. Rev. D **53**, 4991 (1996).
[2] V. Kiselev, A. Kovalsky, and A. Likhoded, Nucl. Phys. **B585**, 353 (2000).
[3] C.-H. Chang, S.-L. Chen, T.-F. Feng, and X.-Q. Li, Phys. Rev. D **64**, 014003 (2001).
[4] A. Abulencia *et al.* (CDF Collaboration), Phys. Rev. Lett. **97**, 012002 (2006).
[5] V. M. Abazov *et al.* (D0 Collaboration), Phys. Rev. Lett. **102**, 092001 (2009).
[6] A particular charge state implies the conjugate unless explicitly stated.
[7] T. Aaltonen *et al.* (CDF Collaboration), Phys. Rev. Lett. **100**, 182002 (2008).
[8] D. Acosta *et al.* (CDF Collaboration), Phys. Rev. D **71**, 032001 (2005).
[9] A. Sill *et al.*, Nucl. Instrum. Methods Phys. Res., Sect. A **447**, 1 (2000).
[10] T. Affolder *et al.*, Nucl. Instrum. Methods Phys. Res., Sect. A **526**, 249 (2004).
[11] G. Ascoli *et al.*, Nucl. Instrum. Methods, A **268**, 33 (1988).
[12] T. Dorigo *et al.*, Nucl. Instrum. Methods, A **461**, 560 (2001).
[13] J. Beringer *et al.* (Particle Data Group), Phys. Rev. D **86**, 010001 (2012).
[14] M. Cacciari, S. Frixione, M. L. Mangano, P. Nason, and G. Ridolfi, J. High Energy Phys. 07 (2004) 033.
[15] C.-H. Chang, C.-F. Qiao, J.-X. Wang, and X.-G. Wu, Phys. Rev. D **72**, 114009 (2005).
[16] T. Aaltonen *et al.* (CDF Collaboration), Phys. Rev. Lett. **100**, 161802 (2008).
[17] T. Aaltonen *et al.* (CDF Collaboration), Phys. Rev. Lett. **106**, 121804 (2011).